Experimental Neurology 316 (2019) 52–62

Contents lists available at ScienceDirect

Experimental Neurology

journal homepage: www.elsevier.com/locate/yexnr

Research Paper

OCT4B-190 protects against ischemic stroke by modulating GSK-3β/HDAC6

Yanting Chen[a,b,1], Zhengzheng Wu[a,c,1], Xiaolei Zhu[a,b], Meijuan Zhang[a,b], Xuefeng Zang[a], Xiaoxi Li[a], Yun Xu[a,b,*]

[a] Department of Neurology, Drum Tower Hospital, Medical School and The State Key Laboratory of Pharmaceutical Biotechnology, Nanjing University, Nanjing 210008, China
[b] Institute of Brain Science, Nanjing University, Nanjing 210008, China
[c] Department of Neurology, Nanjing Hospital of Chinese Medicine Affiliated to Nanjing University of Chinese Medicine, Nanjing 210001, China

ARTICLE INFO

Keywords:
OCT4B
Cell death
Stroke
GSK-3β
Histone deacetylase 6

ABSTRACT

OCT4 is a key regulator in maintaining the pluripotency and self-renewal of embryonic stem cells (ESCs). Human *OCT4* gene has three mRNA isoforms, termed OCT4A, OCT4B and OCT4B1. The 190-amino-acid protein isoform (OCT4B-190) is one of the major products of OCT4B mRNA, the biological function of which is still not well defined. Recent evidence suggests that OCT4B-190 may function in the cellular stress response. The glycogen synthase kinase-3β (GSK-3β) and histone deacetylase 6 (HDAC6) are also key stress modulators that play critical roles in the ischemic cascades of stroke. Hence, we here further investigated the effects of OCT4B-190 in the experimental stroke, and explored the underlying roles of GSK-3β and HDAC6. We found that OCT4B-190 overexpression enhanced neuronal viability at 24 h after oxygen-glucose deprivation (OGD) treatment. Moreover, in male C57BL/6 mice subjected to transit middle cerebral artery occlusion (MCAO), OCT4B-190 overexpression reduced infarct volume and improved neurological function after stroke. Notably, we found spatio-temporal alterations of GSK-3β and HDAC6 in the ischemic cortex and striatum, which were affected by adenovirus-mediated OCT4B-190 overexpression. OCT4B-190 demonstrated similar impacts on neuronal cultures *in vitro*, downregulating OGD-induced GSK-3β activity and HDAC6 expression. In addition, we found that GSK-3β and HDAC6 were co-expressed in the cytoplasm of neurons, and OCT4B-190 had an effect on interactions between GSK-3β and HDAC6 in neuronal cultures subjected to OGD treatment. These findings suggest that OCT4B-190 exerts neuroprotection in the experimental stroke potentially by regulating actions of GSK-3β and HDAC6 simultaneously, which may be an attractive therapeutic strategy for ischemic stroke.

1. Introduction

Ischemic stroke is one of the major causes of morbidity and mortality worldwide. Contributing factors in ischemic cascades include glutamate excitotoxicity, oxidative stress and inflammation. At present, the only globally-validated approaches for stroke are systemic thrombolysis and mechanic recanalization, the utility of which are constrained by narrow treatment time window and the risk of causing cerebral hemorrhage. Consequently, limited number of stroke patients have the chance to receive this effective treatment. It is therefore important to explore novel therapeutic targets and develop new approaches aimed at neuroprotection with a broader time window, which can be used for a much larger fraction of stroke patients (Baxter et al., 2014; Chen et al., 2014; George and Steinberg, 2015).

Human *OCT4* gene has three mRNA isoforms, termed OCT4A, OCT4B, and OCT4B1. OCT4B mRNA has been identified to encode at least three protein isoforms by alternative translation initiation, including the 265-amino-acid protein isoform OCT4B-265, the 190-amino-acid protein isoform OCT4B-190, and the 164-amino-acid protein isoform OCT4B-164 (Gao et al., 2012; Wang et al., 2009). Emerging evidence suggests that OCT4 isoforms have a pivotal regulatory role in diverse biological activities (Guo et al., 2008; Radzisheuskaya and Silva, 2014; Villodre et al., 2016). OCT4A has been generally recognized as a key transcription factor in maintaining the pluripotency and self-renewal of embryonic stem cells (ESCs) (Guo et al., 2008; Radzisheuskaya and Silva, 2014; Villodre et al., 2016). Recently, more attentions have been drawn to the biological functions of OCT4B isoforms, which are mainly localizing in the cytoplasm. Several studies

* Corresponding author at: Department of Neurology, Drum Tower Hospital, Medical School of Nanjing University, 321 Zhongshan Road, Nanjing City, Jiangsu Province 210008, China.
E-mail address: xuyun20042001@aliyun.com (Y. Xu).
[1] Yanting Chen and Zhengzheng Wu contributed equally to this work.

https://doi.org/10.1016/j.expneurol.2019.04.005
Received 4 January 2019; Received in revised form 25 March 2019; Accepted 10 April 2019
Available online 11 April 2019
0014-4886/

suggest OCT4B proteins are potentially responsible for cellular stress response (Gao et al., 2012; Wang et al., 2009). For instance, OCT4B-190 has been reported to be upregulated under cell stress conditions. Endogenous expression of OCT4B-190 was found after heat shock and oxidative stress treatments in human ESCs and several tumor cell lines. Furthermore, overexpression of OCT4B-190 could resist cell apoptosis induced by heat shock (Wang et al., 2009). Further investigations are needed to delineate the biological activities of OCT4B isoforms in different cells and disease models.

Glycogen synthase kinase 3β (GSK-3β) is a cytoplasmic serine/threonine kinase that plays an important role in multiple cellular processes including cellular survival and apoptosis signaling. GSK-3β is broadly distributed in the brain tissue, and can be activated during the brain ischemia (Rana and Singh, 2018). Accumulating evidence indicates that increased GSK-3β activity results in neuronal loss, and contributes to pathogenesis of ischemic stroke (Hanumanthappa et al., 2014). Specific inhibition of GSK-3β has shown neuroprotection *via* reducing the oxidative stress and inflammation in cerebral ischemia/reperfusion (Rana and Singh, 2018). Therefore, modulation of GSK-3β is a promising strategy for ischemic neuroprotection.

Intriguingly, several recent studies demonstrated synergistic neuroprotective effects of GSK-3β inhibition and histone deacetylases (HDACs) inhibitors (Chen et al., 2010; Leng et al., 2008). HDACs are enzymes that deacetylate lysine residues from histones as well as from other non-histone proteins. Accumulating evidence has shown that multiple inhibitors of HDACs exert neuroprotection in the stroke models (Baltan et al., 2011; Langley et al., 2009; Lin et al., 2017; Patnala et al., 2017). HDAC6 is the best-characterized class IIb HDACs that can be regulated by GSK-3β phosphorylation (Chen et al., 2010). HDAC6 may serve as a critical stress and redox regulator (Parmigiani et al., 2008; Ryu et al., 2017). In addition, it has been demonstrated that HDAC6 might be implicated in many critical biological events of the ischemic cascades (Liesz et al., 2013). Selective HDAC6 inhibitors are an emerging class of pharmaceuticals due to the involvement of HDAC6 in a broad spectrum of diseases (Ganai, 2017; Rivieccio et al., 2009; Wang et al., 2018). Our previous study has demonstrated that HDAC6 expression was induced in the ischemic brain (Chen et al., 2012). Selective inhibition of HDAC6 could alleviate stroke-induced neuronal death, brain infarction and functional deficits *in vitro* and *in vivo* (Chen et al., 2012; Wang et al., 2016).

On the basis of these observations, we attempted to investigate the biological functions of OCT4B-190 in the stroke setting *in vitro* and *in vivo*. Furthermore, tentative studies were aimed to reveal the effects of OCT4B-190 on the GSK-3β and HDAC6, which might be promising molecular targets for the synergistic neuroprotection strategy.

2. Materials and methods

2.1. Adenovirus-mediated OCT4B-190 injection and the mouse stroke model

Adenovirus containing the coding sequence of OCT4B-190 (the start codons of OCT4B-265 and OCT4B-164 were mutated) was kindly provided by Professor Jianwu Dai at Chinese Academy of Sciences (Beijing, China). The animal study was conducted in accordance with National Regulations of Experimental Animal Administration and all the experimental protocols performed on animals were approved by the Committee of Experimental Animal Administration of Nanjing University. Male C57BL/6 male mice (body weight 25–30 g) were provided by the Animal Center of Nanjing Drum Tower Hospital.

Mice were anesthetized with sodium pentobarbital (1%) intraperitoneally at a dose of 45 mg/kg, and 3 μl control adenovirus or Ad-OCT4B-190 suspension (1.5 × 10^10 plaque forming units/ml) was injected into the lateral ventricle (0.3 mm posterior from the bregma, 1.0 mm lateral and 3.0 mm in depth). Mice were randomly assigned to each treatment group during the injection process.

The mouse transient middle cerebral artery occlusion (MCAO) procedures were performed as previously described (Chang et al., 2011). In brief, a midline cervical incision was made under a dissecting microscope; the right common carotid artery and external carotid artery (ECA) were isolated. A 6–0 monofilament nylon suture with heat-rounded tip was introduced into a wedge-shaped incision on the ECA and advanced to obstruct the origin of the middle cerebral artery. After 90 min of occlusion, reperfusion was initiated by filament withdrawal. Sham-treated mice were subjected to the same procedure without MCAO. During the procedure, rectal temperature was maintained at 37 ± 0.5 ˚C.

2.2. Behavior test

Neurological deficit after MCAO was evaluated by modified Neurological Severity Scores (mNSS) as described previously (Chang et al., 2011) at 24 h and 72 h after MCAO. The inspectors were masked to grouping of the experimental mice. According to the mNSS, neurological function was graded on a scale of 0 to 18 points. One point was awarded for the inability to perform the tasks or for the lack of a tested reflex.

2.3. Measurement of infarct size

The brain tissues were harvested after 24 h and 72 h of reperfusion. Five 2 mm-thick coronal sections in each brain were prepared for staining using 2,3,5-triphenyltetrazolium chloride (TTC) (Sigma, Saint Louis, MO, USA) in saline (Chang et al., 2011). Slices were photographed with a computer-controlled digital camera (Olympus, Japan) and infarct size was calculated by the image analysis software (Image Pro Plus 6.0; Media Cybernetics, Silver Spring, MD, USA). To rule out the effect of brain edema, the value of infarct volume was provided as a percentage of the contralateral hemisphere.

2.4. Real- time polymerase chain reaction (PCR)

Total RNA was prepared from mouse brain tissue using Trizol reagent (Invitrogen, Camarillo, CA). The cDNA was synthesized using a Prime Script RT reagent kit (Takara, Clontech, USA). Real- time PCR was performed using SYBR Green (Takara, Clontech, USA) with the ABI 7500 PCR instrument (Applied Biosystems, Foster City, CA, USA) as previously described (Chen et al., 2017). The primer sequences used in this study were as follows:

GAPDH forward primer, 5'-GCCAAGGCTGTGGGCAAGGT-3′;
GAPDH reverse primer, 5'-TCTCCAGGCGGCACGTCAGA-3′;
OCT4B forward primer, 5′- GCAGGCCCGGAAGAGA-3′;
OCT4B reverse primer, 5′- GGGCTTCGGGCACTTC-3′.

2.5. Western blotting

To analyze protein levels of HDAC6, GSK-3β and α-tubulin, mice in each group were sacrificed, and then cortical and striatum tissue were dissected from ipsilateral hemispheres of the mice subjected to 90 min MCAO followed by 3 h and 24 h of reperfusion. The procedure was described previously (Chen et al., 2012). Equal amounts of protein samples were separated by SDS–PAGE and blotted onto polyvinylidene fluoride (PVDF) membranes. The membranes were probed with primary antibodies against HDAC6 (1:500, BioWorld), p-HDAC6 (1:500, Affinity Biosciences), GSK-3β (1:1000, Cell Signaling), p-GSK-3β (1:1000, Cell Signaling), α-tubulin (1:2000, Cell Signaling), Aceylated α-tubulin (1:2000, Abcam), GAPDH (1:5000, BioWorld). The α-tubulin and GAPDH were used as the loading control. The proteins were detected using horseradish peroxidase-conjugated anti-rabbit or anti-mouse secondary antibodies and visualized using chemiluminescence reagents provided with the ECL kit (Bio-Rad, Hercules, CA, USA). All

samples were normalized to the α-tubulin and then normalized to the sham control for all semi-quantitative comparisons.

2.6. Co-immunoprecipitation assay

Proteins of primary neurons were used for co-immunoprecipitation assay (Zhu et al., 2013). The lysate was preincubated for 1 h at 4 °C with 25 μl of protein G-sepharose beads (Sigma-Aldrich) and then centrifuged to remove proteins that adhered nonspecifically to the beads and obtained the target supernatant for following IP experiment. The supernatant was rotated overnight at 4 °C with anti-HDAC6 antibody (2 μg/500 μg protein, Santa Cruz, CA, USA) and protein G-sepharose beads were added the following morning. The immune complexes were isolated by centrifugation, and were washed and boiled for 5 min in loading buffer. Proteins were analyzed by western blotting as described above.

2.7. Immunostaining

Details of immunostaining protocols could be found in our previous publications (Chen et al., 2015; Zhu et al., 2014). Primary neuronal cultures were fixed in 4% formaldehyde and incubated overnight with primary antibodies HDAC6 (1:500, Abcam) and GSK-3β (1:1000, Cell Signaling). Antibody binding was visualized with fluorescently-tagged secondary antibodies (1:500, Invitrogen) and fluorescent images were taken using a confocal laser-scanning microscope (Olympus, Japan).

2.8. Primary cortical neuronal culture

Primary cortical neurons were cultured from E16–17 mouse embryo as described previously (Chen et al., 2012). Briefly, cortexes of the fetus were dissected and treated with trypsin to prepare cell suspension. Cells were plated at 5 × 105 cells/ml on 12 well or 96 well poly-D-lysine-coated plates. Cells were grown in Neurobasal media supplemented with B27 (Invitrogen, Carlsbad, California, USA) and 25 nM glutamine at 37 °C in a humidified 5% CO_2 incubator.

2.9. Oxygen-glucose deprivation (OGD)

Cortical cultures were subjected to OGD to simulate ischemia *in vitro* (Chen et al., 2012). Briefly, cultures were switched from the normal culture medium to the oxygen-depleted, glucose-free medium. Cells were incubated in a hypoxia chamber previously flushed for 15 min with 5%CO2/95%N2 at 2 psi (1 psi = 6.89 kPA). Valves were closed and chambers were incubated at 37 °C for 1 h. Then, cells were returned to normal culture condition for later treatment.

2.10. MTT assay

The neuronal viability was determined by 3-(4,5-dimethylthiazol-2-yl)-2,5-diphenyl-tetrazolium bromide (MTT) assay (Chen et al., 2012). In brief, cell culture medium in 96-well plates was aspirated and replaced with fresh neuron feeding medium containing 0.5 mg/ml MTT (Sigma, Saint Louis, MO, USA) for 4 h at 37 °C. The formazan crystals were dissolved in 100 μl of DMSO and the absorbance was measured using an ELISA plate reader (TECAN, Switzerland). Cell survival rates were expressed in percentage of the value of control adenovirus treatment group (normal controls).

2.11. Statistical analysis

Comparisons between groups were carried out by one-way analysis of variance (ANOVA) followed by Bonferroni-corrected post-hoc tests. Comparative differences were considered significant at $P < .05$. The statistical software package SigmaStat 11.5 (SPSS) was used to perform all analysis. Data are presented as means ± SEM.

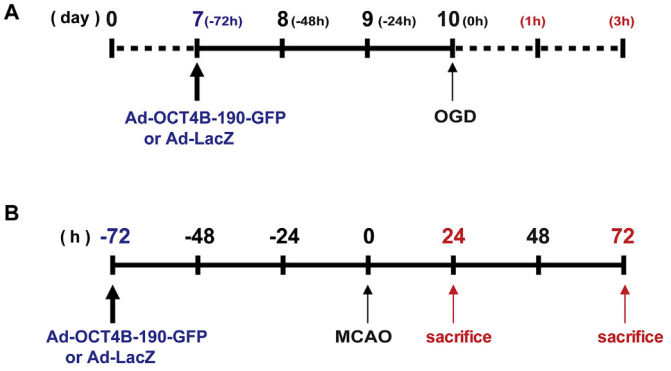

Supplementary Fig. 1. The diagram of OCT4B-190 administration *in vitro* and *in vivo*. A. Primary neurons were cultured for 7 days and treated with OCT4B-190-GFP adenovirus. After 3 days of infection, the neuronal cultures were subjected to OGD treatment. The effects of OCT4B-190 were examined 1 h and 3 h after OGD. B. Ad-OCT4B-190 was administrated 72 h before MCAO and effects of OCT4B-190 overexpression on ischemic brain damage were investigated by evaluating neurologic deficit and infarct volume at 24 h and 72 h after stroke.

3. Results

3.1. OCT4B-190 overexpression protects against ischemic brain injury in vitro and in vivo

Given that OCT4B-190 has been identified to participate in cellular stress as mentioned above (Wang et al., 2009), we were interested in exploring whether OCT4B-190 could have effects on neuronal cell death in the *in vitro* stroke model. We first examine the transfection efficiency of OCT4B-190 containing adenovirus in primary neurons. Primary neurons were cultured for 7 days and treated with OCT4B-190-GFP adenovirus (Supplementary Fig. 1A). As shown in Fig. 1A, an intense green GFP signal at 3 days after infection was found in neuronal cultures, indicating an efficient OCT4B-190 overexpression in primary neurons *via* this adenovirus vector. Following MTT assay demonstrated a substantial decline of neuronal viability at 3 h after OGD treatment, and OCT4B-190 overexpression could promote neuronal survival in a concentration-dependent manner ($P < .01$) (Fig. 1B and Supplementary Fig. 2).

Using real- time PCR assay, we detected OCT4B expression in the mouse ischemic cortex within 7 days after MCAO. A minor increase of OCT4B mRNA expression was induced at 1 day after MCAO, which peaked at 3 days and was persistent within 7 days after MCAO (Supplementary Fig. 3). These results indicated that an endogenous OCT4B could be induced in the ischemic brain tissue after stroke. To further verify neuroprotective effects of OCT4B-190 *in vivo*, we first evaluated the efficiency of gene expression of adenoviral administration through the ventricular route in this study. Ad-OCT4B-190 containing GFP gene was infused into the right lateral ventricle of normal mice, and Ad-OCT4B-190 expression was confirmed by detecting GFP fluorescence 72 h after Ad-OCT4B-190 administration. Using this method, we have shown highly localized and robust GFP expression in the cells surrounding the right ventricular region in the brain slices as early as 72 h post-injection (Fig. 2A). Thus, intraventricular infusion of recombinant adenovirus was efficacious in overexpression of OCT4B-190. For the following studies, Ad-OCT4B-190 or Ad-LacZ (control adenovirus) was administrated 72 h before MCAO and effects of OCT4B-190 overexpression on ischemic brain damage were investigated by evaluating neurologic deficit and infarct volume at 24 h and 72 h after stroke (Supplementary Fig. 1B). We found that compared to MCAO mice with Ad-LacZ pretreatment, MCAO mice with OCT4B-190 overexpression had improved neurological function at 72 h after stroke (72 h: 9.6 ± 0.9 *vs.* 6.0 ± 0.8, $P < .05$) (Fig. 2B). Consistently, OCT4B-190

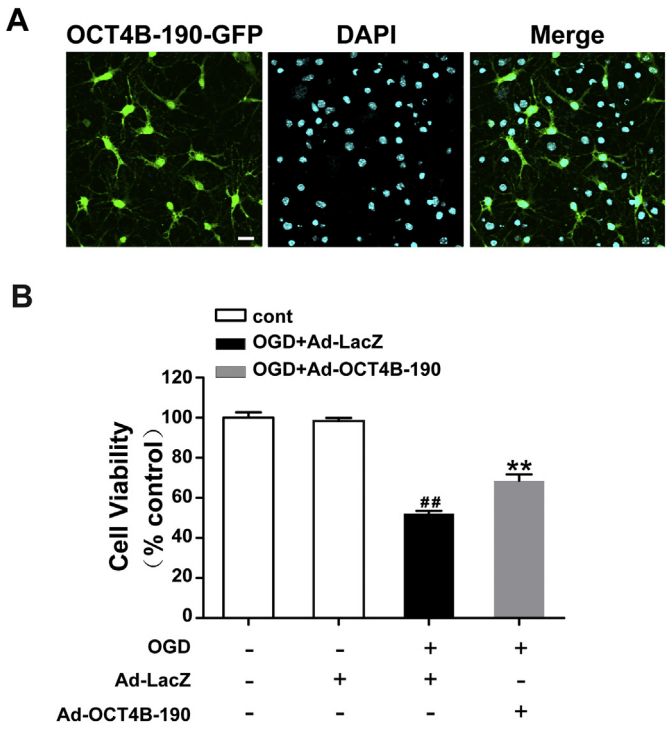

Fig. 1. Protective effects of OCT4B-190 on OGD-induced neuronal death. A. Primary cortical neurons showed an intense GFP signal (green) at 3 days after infection with adenovirus containing OCT4B-190-GFP. Scale bar represents 20 μm. B) OCT4B-190 overexpression enhanced neuronal viability after OGD treatment. Primary cortical neurons were infected with adenovirus expressing OCT4B-190 or control adenovirus for 3 days, then neurons were subjected to 30 min of OGD treatment, 3 h after which cell viability was examined by MTT assay. Data are presented as means ± SEM. ($n = 6$), $^{\#\#}P < .01$ *vs.* control group, $^{**}P < .05$ *vs.* OGD + Ad-LacZ. (For interpretation of the references to colour in this figure legend, the reader is referred to the web version of this article.)

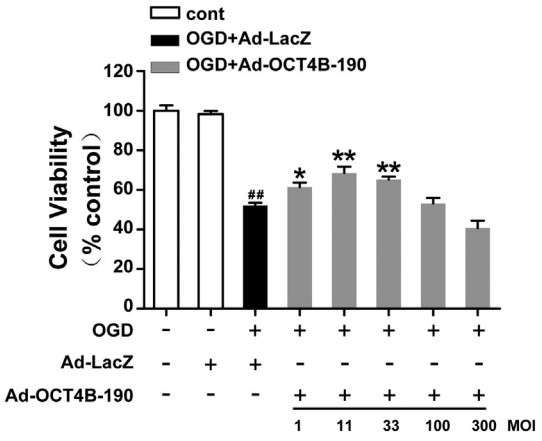

Supplementary Fig. 2. Adenovirus containing OCT4B-190 protected against OGD-induced neuronal death. Preliminary study of OCT4B-190 on neuronal viability after OGD treatment. MTT assay showed a concentration-dependent effects of OCT4B-190 adenovirus on neuronal viability at different multiplicity of infection (MOI). A concentration of 11 MOI was used for the following *in vitro* studies. ($n = 6$), $^{\#\#}P < 0.01$ *vs.* control group, $^{*}P < 0.05$ and $^{**}P < 0.01$ *vs.* OGD + Ad-LacZ.

overexpression apparently reduced the infarct volume of MCAO mice at 24 h post stroke, and also moderately mitigated the infarct size at 72 h after ischemia (24 h: 37.6 ± 2.9% *vs.*17.0 ± 2.3%, $P < .01$; 72 h: 42.7 ± 3.3% *vs.* 34.9 ± 2.5%, $P < .05$) (Fig. 2C, D).

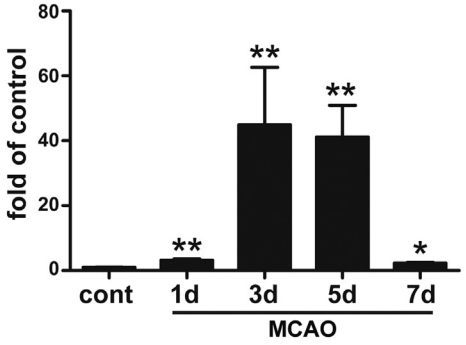

Supplementary Fig. 3. Time course expression of OCT4B mRNA after ischemic stroke. Male C57BL/6 mice were subjected to transient MCAO. Using RT-PCR asssay, the mRNA expression of OCT4B was determined at different time points within 7 days after MCAO treatment. Data are presented as means ± SEM, ($n = 3$–6), $^{*}P < 0.05$ *vs.* MCAO + Ad-LacZ, $^{**}P < 0.01$ *vs.* MCAO + Ad-LacZ.

3.2. OCT4B-190 overexpression attenuates stroke-induced GSK-3β activation

Based on the neuroprotective effects of OCT4B-190 in stroke models and potential roles of OCT4B-190 in cell stress, we hypothesized that OCT4B-190 might regulate key mediators associated with neuronal death and pathogenesis of ischemic brain damage. GSK-3β has been well recognized to play key roles in cellular processes and associated with the ischemic cascades (Hanumanthappa et al., 2014). To investigate whether GSK-3β was involved in the beneficial effects of OCT4B-190 in the mouse experimental stroke, GSK-3β activity was evaluated by western blotting at 3 h and 24 h after MCAO treatment in either Ad-OCT4B-190 or Ad-LacZ pretreated group. As shown in Fig. 3A, both cortical p-GSK-3β and GSK-3β were elevated in MCAO mice at 3 h after reperfusion, with no evident alteration of GSK-3β activity (indicated by p-GSK-3β/GSK-3β ratio). GSK-3β activity in the ischemic cortex was downregulated at 24 h of reperfusion ($P < .01$), with a higher ratio of p-GSK-3β/GSK-3β. OCT4B-190 overexpression could inhibit GSK-3β activity in the mouse ischemic cortex at both 3 h and 24 h after MCAO treatment ($P < .01$). However, a distinct change pattern of GSK-3β activity was observed in the ischemic striatum. A pronounced GSK-3β activity was induced in the ischemic striatum at both 3 h and 24 h after stroke, which could be effectively reversed by OCT4B-190 overexpression ($P < .01$) (Fig. 3).

3.3. OCT4B-190 overexpression inhibits HDAC6 expression after stroke

Accumulating evidence suggests HDAC6 exerts diverse activities including regulation of cellular stress (Matthias et al., 2008), and acts as a promising target for neuroprotective therapeutics in ischemic stroke. Therefore, the concurrent influence of OCT4B-190 in the alteration of HDAC6 after cerebral ischemia was likewise verified. It was interesting to note that ischemic stroke induced a region-specific alteration of HDAC6. In the ischemic cortex, HDAC6 expression was significantly increased as early as 3 h after reperfusion ($P < .01$). On the contrary, no induction of HDAC6 expression after stroke was detected in the striatum (Fig. 4A), whereas ischemic stroke resulted in a substantial reduction of striatal HDAC6 at 24 h time point ($P < .05$) (Fig. 4B). Notably, OCT4B-190 treatment could robustly suppress HDAC6 levels in the ischemic cortex and striatum by simultaneously ($P < .01$) (Fig. 4). To confirm whether HDAC6 activity was involved in the OCT4B-190 actions in the ischemic stroke, the protein levels of α-tubulin, a classical protein substrate of HDAC6, was determined to reflect HDAC6 activity. There was no dominant alteration of HDAC6 activity detected in the ischemic brain tissue. In addition, OCT4B-190 had no effects on HDAC6 activity after stroke (Supplementary Fig. 4).

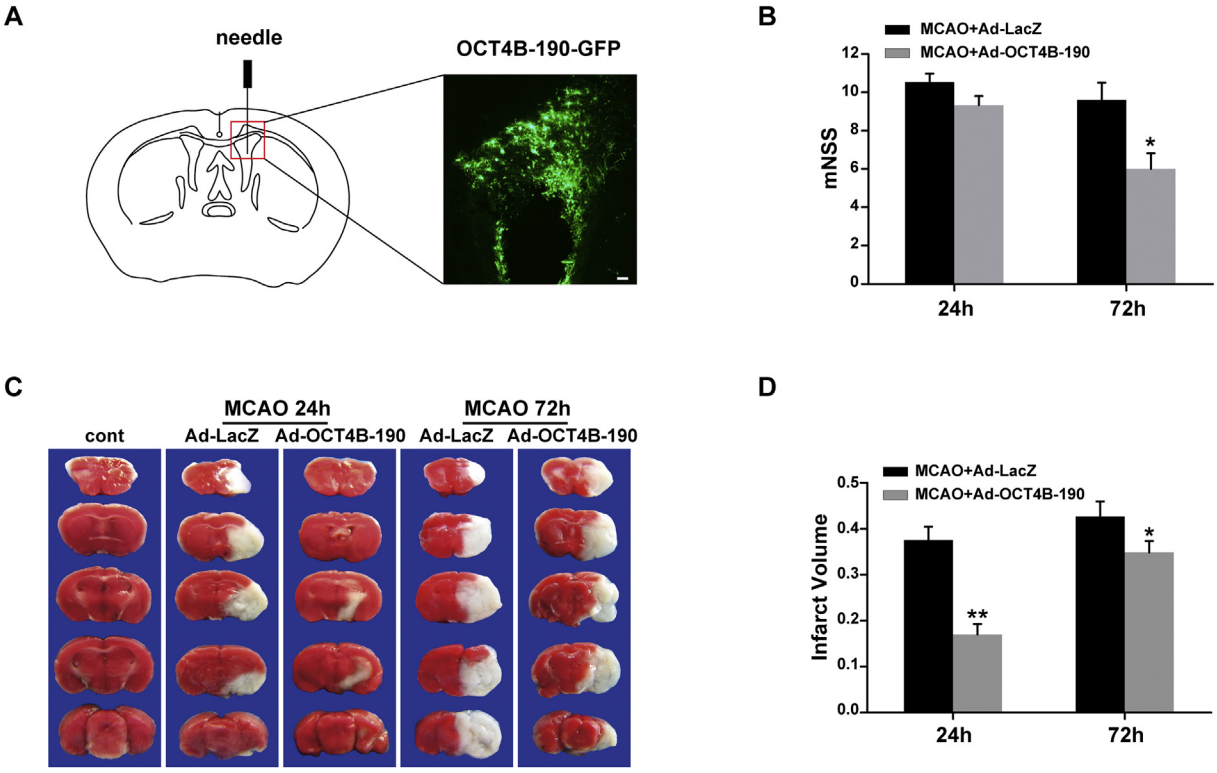

Fig. 2. Neuroprotection of OCT4B-190 in the mouse experimental stroke. Male C57BL/6 mice were subjected to transient MCAO after adenovirus Ad-LacZ or Ad-OCT4B-190-GFP pretreatment. A. Schematic of ventricle-targeted delivery of an adenovirus encoding OCT4B-190-GFP and representative image of OCT4B-190 distribution in the mouse brain. Adenovirus containing OCT4B-190-GFP was injected into the right ventricle. Immunofluorescence indicated a robust OCT4B-190 expression (green) surrounding the ventricle. Scale bar represents 50 μm. B. OCT4B-190 overexpression alleviated neurological deficits of MCAO mice. (n = 6–10), $^{*}P < 0.05$ *vs.* MCAO + Ad-LacZ. C. Representative images of TTC staining showing OCT4B-190 overexpression reduced infarct volume of MCAO mice. D. Quantification of infarct volume. Data are presented as means ± SEM. (n = 4–6), $^{*}P < 0.05$ and $^{**}P < 0.01$ *vs.* MCAO + Ad-LacZ. (For interpretation of the references to colour in this figure legend, the reader is referred to the web version of this article.)

3.4. OCT4B-190 overexpression modulates the neuronal interaction of GSK-3β with HDAC6

To determine whether OCT4B-190 overexpression could affect neuronal GSK-3β activity and HDAC6 after stroke *in vitro*, immunoblotting was also used to detect the GSK-3β and HDAC6 levels in primary neurons after OGD treatment. As shown in Fig. 5A, GSK-3β was significantly activated at both 1 h and 3 h after OGD treatment, with a reduced p-GSK-3β/GSK-3β ratio ($P < .01$). OCT4B-190 overexpression demonstrated a prominent inhibitory effect on GSK-3β activity in OGD-treated neuronal cultures at 3 h after reperfusion ($P < .01$), consistent with the findings in the MCAO mice. In addition, neuronal HDAC6 was elevated immediately at 1 h after OGD treatment, which was effectively downregulated by OCT4B-190 overexpression ($P < .01$) (Fig. 5B). Consistently, no evident change of HDAC6 activity was found in the neuronal cultures after OGD treatment, and OCT4B-190 did not affect neuronal HDAC6 activity (Supplementary Fig. 5). Sequent immunofluoresence assay revealed co-expression of GSK-3β and HDAC6 in neuronal cytoplasm *in vitro* (Fig. 6A and Supplementary Fig. 6). Using Co-Immunoprecipitation, we found that GSK-3β interacted with HDAC6 to a lesser extent in the normal neuron cultures. Whereas, a more intimate interaction of activated GSK-3β with HDAC6 was found in OGD neuronal cultures, and OCT4B-190 overexpression tended to dissociate this molecular interaction ($P < .01$) (Fig. 6B). Furthermore, normal neurons were treated with AKT inhibitor VII to induce the activation of GSK-3β (Chen et al., 2010). It was found that AKT inhibitor treatment robustly suppressed the phosphorylation of GSK-3β in the neuronal cultures, indicating the activation of GSK-3β. However, AKT inhibitor treatment decreased the level of p-HDAC6 in neuronal cultures (Supplementary Fig. 7A). In addition, the level of p-HDAC6 was not affected by OCT4B-190 overexpression either in the normal neuronal cultures or AKT inhibitor-treated neuronal cultures (Supplementary Fig. 7B).

4. Discussion

This work gives an insight into the novel biological effects of OCT4B-190 in the transient ischemic stroke disease models. It is worthy to note that overexpression of OCT4B-190 protects against neuronal death and ischemic brain damage. In addition, cellular stress associated GSK-3β and HDAC6 were identified as key mediators involved in the neuroprotection of OCT4B-190 in the ischemic stroke.

The *OCT4* gene with diverse transcription and translation products has possessed multiple biological functions. OCT4B proteins have been shown to play a crucial role in cell stress and apoptosis (Gao et al., 2012; Wang et al., 2009). A putative internal ribosome entry site (IRES) has been identified to be existing in the OCT4B mRNA, which might account for synthesis of OCT4B proteins under stress conditions (Rajanahalli et al., 2015; Wang et al., 2009). Several recent studies indicated OCT4B was reactivated in cancer cells, and could contribute to regulation of apoptosis and cell death, mediating oncogenesis in cancer dissemination (Lin et al., 2019; Meng et al., 2018). OCT4B-265 was demonstrated to be upregulated under genotoxic stress in stem cells, and functioned in stress response *via* p53 signaling pathway (Gao et al., 2012). OCT4B-190, another major OCT4B isoform, was also verified to be induced in stress conditions and might protect cellular apoptosis under stress (Wang et al., 2009).

After the onset of cerebral ischemia, series of complex pathological processes are initiated to result in cell death and ischemic brain damage (Baxter et al., 2014; Eltzschig and Eckle, 2011; Jung et al., 2010). Given

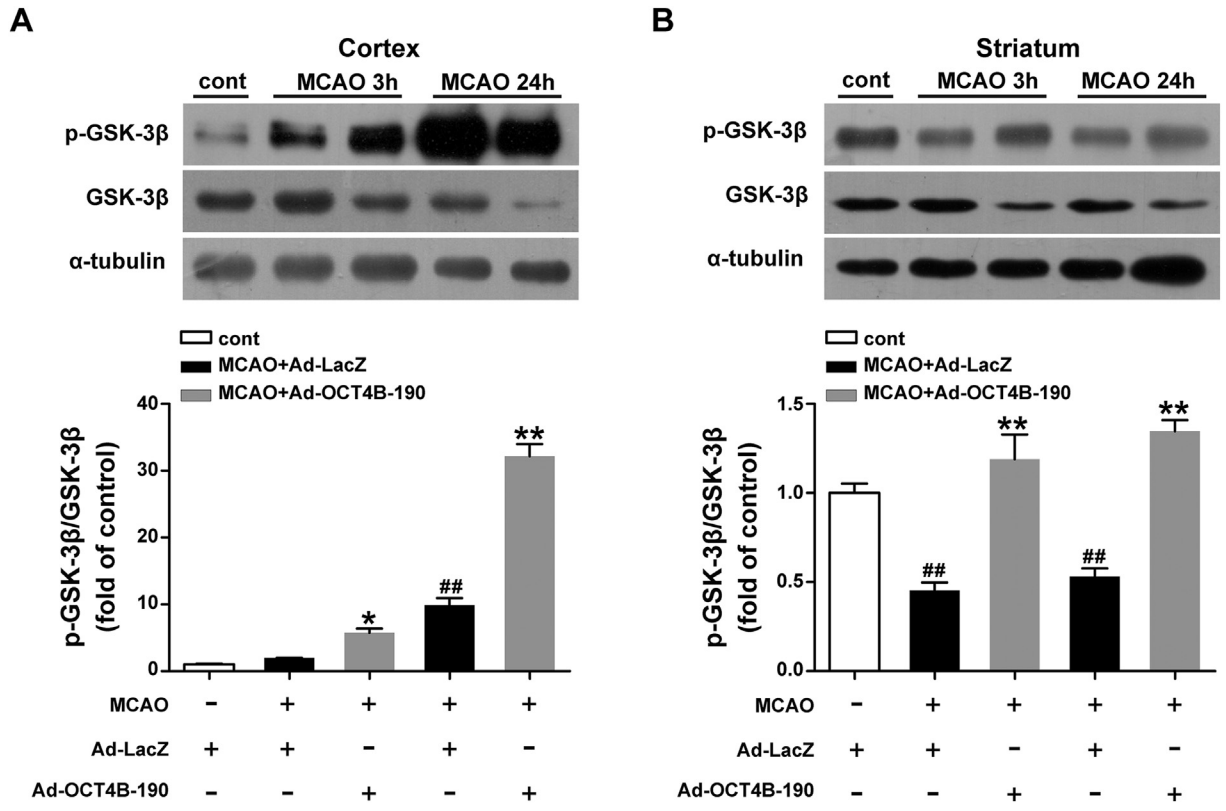

Fig. 3. Inhibitory effects of OCT4B-190 on GSK-3β activity after stroke. Male C57BL/6 mice were subjected to transient MCAO after Ad-LacZ or Ad-OCT4B-190-GFP pretreatment. GSK-3β activity was evaluated by western blotting 3 h and 24 h after MCAO treatment. A, B. Representative immunoblot of GSK-3β and p-GSK-3β from cortex or striatum. C, D. Statistics results showed that OCT4B-190 overexpression enhanced the ratio of p-GSK-3β/GSK-3β in both cortex and striatum after MCAO. Data are presented as means ± SEM. (n = 4–6), $^{\#\#}P < .01$ *vs.* sham + Ad-LacZ, $^{*}P < .05$ and $^{**}P < 0.01$ *vs.* MCAO + Ad-LacZ.

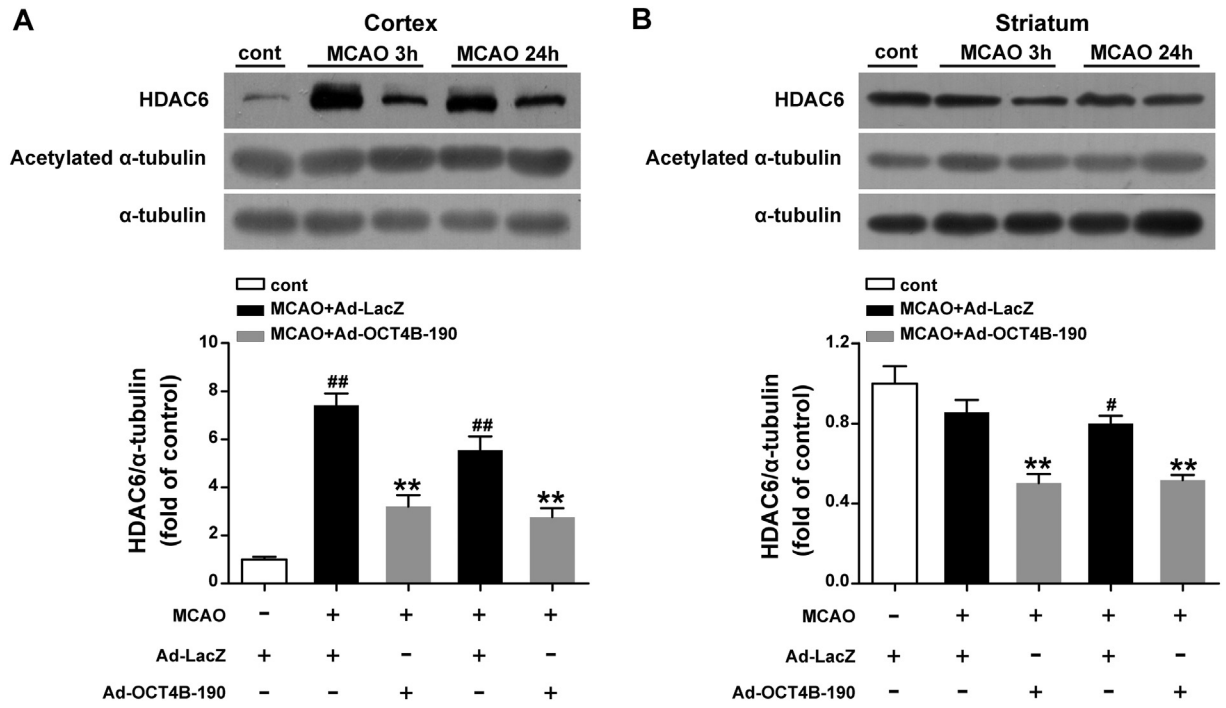

Fig. 4. Suppression of HDAC6 expression by OCT4B-190 after stroke. Male C57BL/6 mice were subjected to transient MCAO after Ad-LacZ or Ad-OCT4B-190-GFP pretreatment. HDAC6 expression was evaluated by western blotting 3 h and 24 h after MCAO treatment. A, B. Representative immunoblotting of HDAC6 and α-tubulin from cortex or striatum. C, D. Statistics results showed that OCT4B-190 overexpression suppressed HDAC6 expression in either cortex or striatum of MCAO mice. Data are presented as means ± SEM. (n = 4–6), $^{\#\#}P < .01$ *vs.* sham + Ad-LacZ, $^{**}P < 0.01$ *vs.* MCAO + Ad-LacZ.

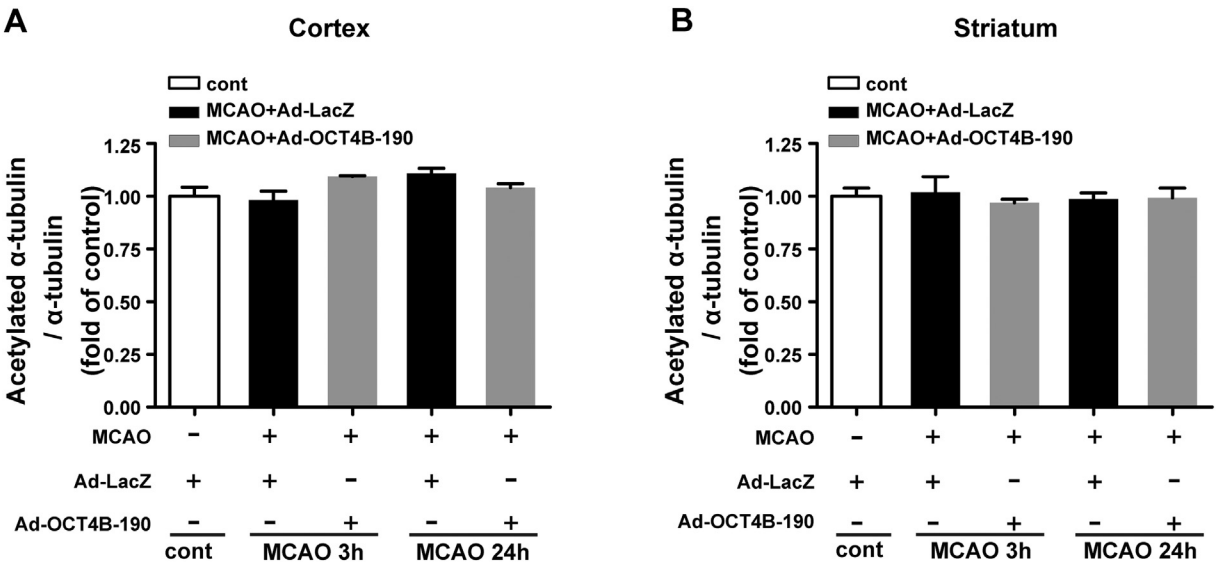

Supplementary Fig. 4. No alteration of α-tubulin acetylation after stroke *in vivo*. Male C57BL/6 mice were subjected to MCAO after adenovirus Ad-LacZ or Ad-OCT4B-190-GFP pretreatment. The expression of α-tubulin and acetylated α-tubulin were evaluated by western blotting 3 h and 24 h after MCAO treatment. A. Statistics results showed that acetylation of α-tubulin was not affected by OCT4B-190 in the cortex of MCAO mice. B. Statistics results showed that acetylation of α-tubulin was not affected by OCT4B-190 in the striatum of MCAO mice. Each protein expression level determined by western blotting was shown relative to that of sham-operated mice. Data are presented as means ± SEM, (n = 4–6).

that potential anti-apoptosis properties of OCT4B-190 isoform, we further explore the biological functions of OCT4B-190 in the cellular and disease models of ischemic stroke. We found that OCT4B-190 overexpression could prominently protect against neuronal damage subject to OGD treatment, a cellular stroke model *in vitro* (Fig. 1). In addition, contralateral delivery of OCT4B-190 apparently alleviated ischemic brain damage of the MCAO mice (Fig. 2). These findings revealed that OCT4B-190 had neuroprotective effects in the experimental stroke.

GSK-3β is critical in regulating multiple biological events including neuronal viability. Emerging evidence suggests that GSK-3β could be activated and contribute to neuronal death and pathologenesis of

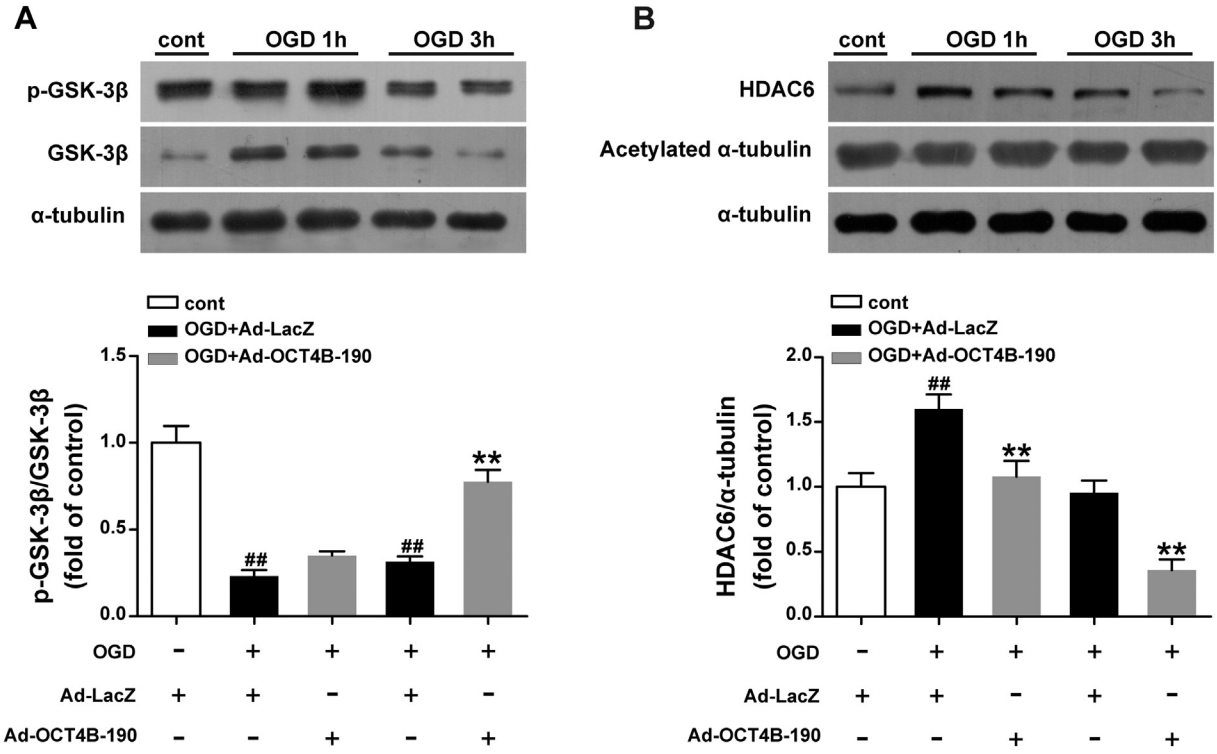

Fig. 5. Regulation of OCT4B-190 in GSK-3β and HDAC6 after stroke *in vitro*. Primary cortical neurons were infected with adenovirus expressing OCT4B-190 or control adenovirus for 3 days, then neurons were subjected to 30 min of OGD treatment, 1 h and 3 h after which the expression of GSK-3β and HDAC6 was examined by western blotting. A, B. Representative immunoblot of GSK-3β and HDAC6 from primary neuronal cultures. C, D. Statistics results showed that OCT4B-190 overexpression inhibited OGD-induced GSK-3β activity and HDAC6 expression. Data are presented as means ± SEM. (n = 3), $^{\#\#}P < .01$ *vs.* control neuronal cultures, $^{**}P < .01$ *vs.* OGD + Ad-LacZ.

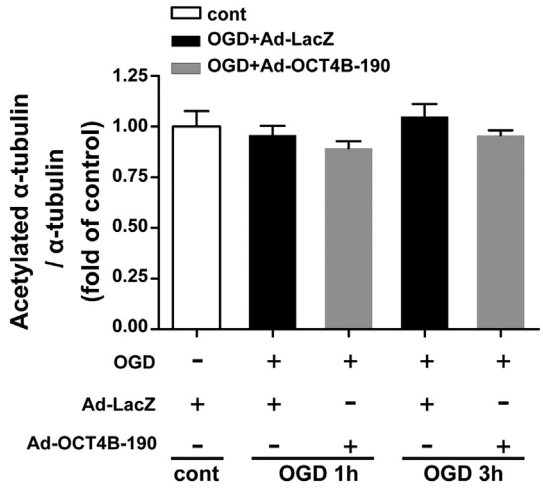

Supplementary Fig. 5. No alteration of α-tubulin acetylation after stroke *in vitro*. Primary cortical neurons were infected with adenovirus expressing OCT4B-190 or control adenovirus for 3 days, then neurons were subjected to 30 min of OGD treatment, 1 h and 3 h after which the expression of α-tubulin and acetylated α-tubulin were examined by western blotting. Statistics results showed that acetylation of α-tubulin was not affected by OCT4B-190 in the OGD-treated neurons. Data are presented as means ± SEM, (n = 3).

ischemic stroke (Rana and Singh, 2018). Many efforts were devoted to explore novel GSK-3β inhibitors with potent activities and excellent brain permeability, which might serve as new promising drugs for neuroprotective treatment in stroke (Khanfar et al., 2010). Consistent with previous observations, we found a remarkable alteration of GSK-3β activity in the ischemic brain tissue and OGD-treated neurons (Fig. 3 and Fig. 6A). Moreover, it was worthy to note that stroke induced a spatio-temporal discrepancy of GSK-3β activity in the ischemic cortex and striatum (Fig. 3). A dominant deactivation of GSK-3β was found in the peri-infarct cortex, whereas early significant activation of GSK-3β was induced in the striatal ischemic core (Fig. 3). Thus, we speculated that GSK-3β might have subtle functions in the pathological processes of cerebral ischemia. The cortical deactivation of GSK-3β could be a self-protective molecular mechanism under ischemic stress condition. However, the striking activation of GSK-3β in the striatum might result from more severe ischemic tissue damage and the compromise of this endogenous neuroprotection. Notably, OCT4B-190 could effectively inhibit GSK-3β activity of ischemic brain tissue and neuronal cultures (Fig. 3 and Fig. 6A). Therefore, we supposed that the inhibition of GSK-3β might to some extent contribute to the neuroprotective actions of OCT4B-190.

HDAC6 plays an important role in stress responses and regulates sensitivity to cell death during oxidative stress and post-stress recovery (Ryu et al., 2017). Inhibition of HDAC6 could increase cellular anti-oxidant activity and protect against oxidative insults by acetylating peroxiredoxins (Parmigiani et al., 2008). HDAC6 has been defined as a potential nontoxic therapeutic target for ameliorating oxidative stress-induced neurodegeneration and insufficient axonal regeneration (Rivieccio et al., 2009). Previous studies showed an early increase of HDAC6 expression in OGD-treated neurons and ischemic cortex of MCAO mice (Chen et al., 2010; Liesz et al., 2013). Our previous *in vitro* study demonstrated that specifically inhibiting HDAC6 could enhance neuronal viability after OGD treatment (Chen et al., 2010). A recent

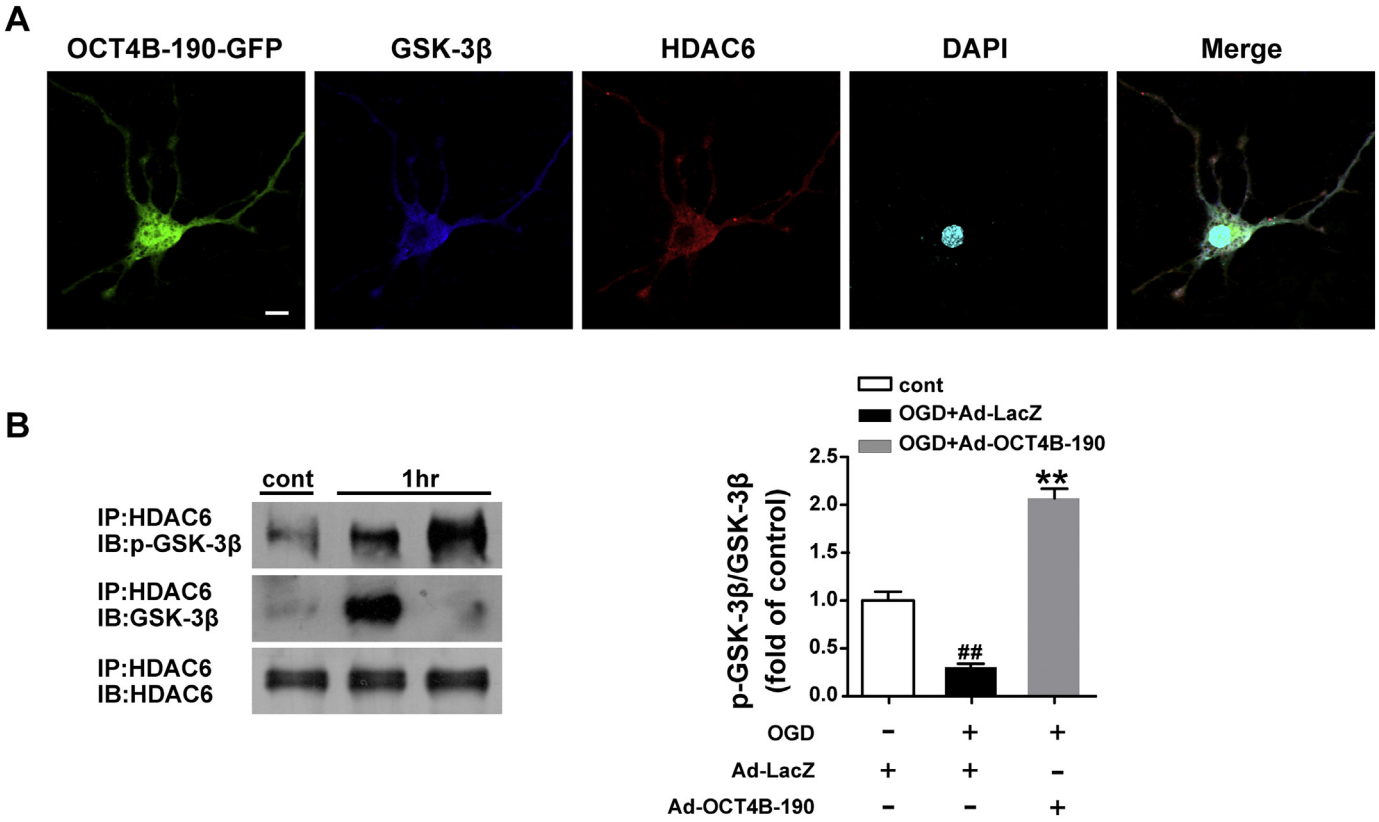

Fig. 6. Modulation of OCT4B-190 in HDAC6 and GSK-3β interactions after stroke *in vitro*. A. Representative immunofluorescence images demonstrated the co-localization of OCT4B-190 (green), GSK-3β (blue) and HDAC6 (red) in primary neuronal cultures. Scale bar represents 5 μm. B. Primary cortical neurons were infected with adenovirus expressing OCT4B-190 or control adenovirus for 3 days, then neurons were subjected to 30 min of OGD treatment, 1 h after which the binding of GSK-3β and HDAC6 was examined. Co-IP assay suggested a direct interaction between GSK-3β with HDAC6 that was affected by OCT4B-190. Data are presented as means ± SEM. (n = 3), $^{\#\#}P < .01$ *vs.* control neuronal cultures, $^{**}P < .01$ *vs.* OGD + Ad-LacZ. (For interpretation of the references to colour in this figure legend, the reader is referred to the web version of this article.)

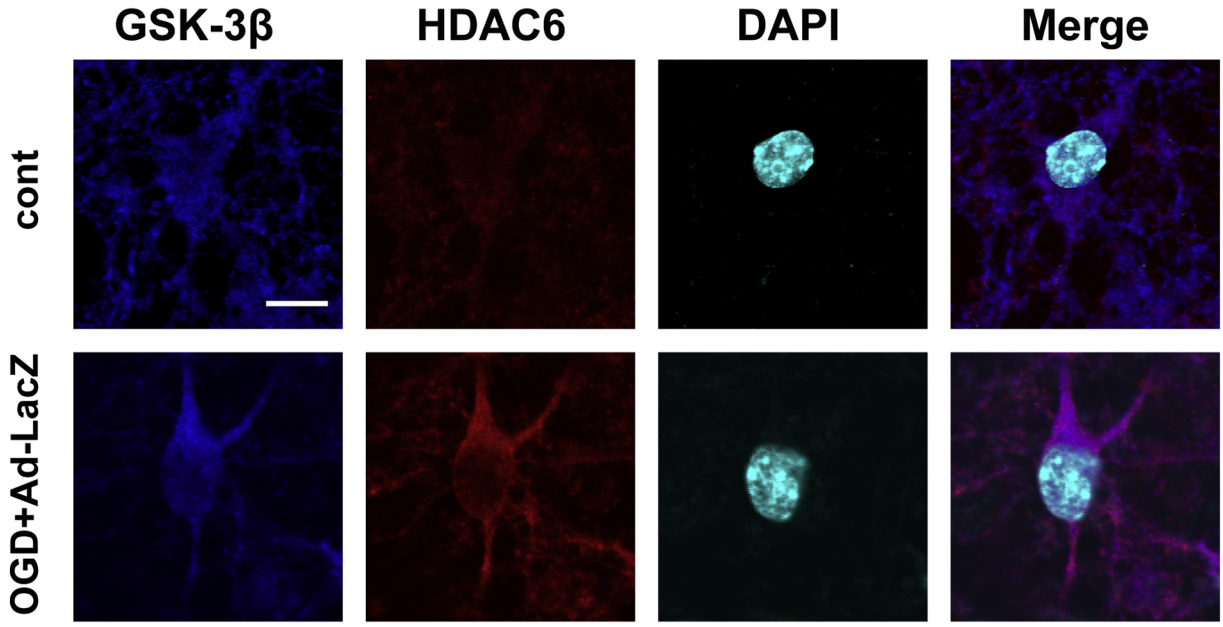

Supplementary Fig. 6. Representative immunofluorescence images demonstrated the co-expression of GSK-3β (blue) and HDAC6 (red) in either control neuronal cultures and OGD neuronal cultures. The naive neurons pretreated with Ad-LacZ was used as control. Scale bar represents 5 μm.

study showed that post-ischemic treatment of tubastatin A, a novel specific HDAC6 inhibitor, robustly improved functional outcomes, reduced brain infarction, and ameliorated neuronal cell death in MCAO rats (Wang et al., 2016). HDAC6 might be involved in a switch from UPS to autophagy, and connected with the function of regulatory T cells following ischemic brain injury (Liu et al., 2018). Based on these findings, we hypothesized HDAC6 might have a sophisticated role in regulating post-stroke pathological events mediating neuronal death and ischemic brain damage. In this study, we consistently confirmed an early upregulation of HDAC6 expression in the OGD-treated neurons and the ischemic cortex, but a downward shift was observed at later time point after reperfusion (Fig. 4A and Fig. 5B). On the contrary, no increase of HDAC6 expression was found in the ischemic striatal core (Fig. 4B). Although the enzymatic activity of HDAC6 seemed to be responsible for many of its biological functions, the role of HDAC6 in our stroke models was likely independent of its tubulin deacetylase activity (Fig. 4 and Supplementary Fig. 4-5). Therefore, HDAC6 turns out to response immediately after ischemic insult, and an early elevation of HDAC6 expression may correlate with mild ischemic damage in the peri-infarct region. OCT4B-190 overexpression could similarly inhibit HDAC6 in the ischemic neurons and brain tissue, resulting in reduced neuronal damage and brain infarct volume, together with improved neurological function (Fig. 1-5). This finding supported that HDAC6 might be an intriguing candidate target for stroke treatment.

Several studies have demonstrated a potential phosphorylation site of GSK-3β in HDAC6 (Borgas et al., 2016; Chen et al., 2010). An interesting relationship between HDAC6 and GSK-3β has been established in the mitochondrial transport of hippocampal neurons (Chen et al., 2010). Activated GSK-3β may activate HDAC6 *via* phosphorylation of serine-22, leading to α-tubulin deacetylation and microtubule disassembly (Borgas et al., 2016). The inhibition of GSK-3β decreased HDAC6-mediated microtubules acetylation and improved mitochondrial transport (Chen et al., 2010). On the contrary, we found that the activation of GSK-3β induced by AKT inhibitor resulted in decreased level of p-HDAC6 in neuronal cultures (Supplementary Fig. 7), which implied that GSK-3β might not be the main phosphorylation kinase of HDAC6. This result was in consistent with the finding of a previous study, which demonstrated that the phosphorylation of HDAC6 was modulated by p38MAPK/AKT (Wu et al., 2016). In addition, in a rat model of transient MCAO and an *in vitro* model of excitotoxicity, specific inhibition of HDAC6 conferred neuroprotection and mitigated impaired FGF-21 signaling in the ischemic hemisphere, including upregulating β-Klotho, and activating ERK and Akt/GSK-3β signaling pathways (Wang et al., 2016). In this study, we found significant alterations of GSK-3β activity in line with the pace of HDAC6 changes following ischemic stroke, which could be simultaneously affected by OCT4B-190 overexpression (Fig. 3-5). Possible correspondences between GSK-3β and HDAC6 after stroke insult were found (Fig. 6). OCT4B-190 might modulate the stroke-induced molecular interactions of GSK-3β and HDAC6, which might be independent of the direct phosphorylation of HDAC6 by GSK-3β (Supplementary Fig. 7).

Given that OCT4B-190 was probably an active player in the cellular stress responses and protected against ischemic brain injury. We considered that other stress modulators such as poly (ADP-ribose) polymerase (PARP)-1, sirtuin 3 (SIRT3) and stress-inducible phosphoprotein 1 (STI1) might be implicated in the actions of OCT4B-190. PARP-1 catalyzes the transfer of ADP-ribose units from NAD^+ to target proteins including histones and transcriptional factors. Accumulating evidence suggests that PARP-1 functions in converging stress signaling pathways. PARP-1 plays crucial roles in modulating genotoxic, oxidative, metabolic and inflammatory stress responses (Luo and Kraus, 2012). Inhibiting PARP-1 could improve neuronal survival and alleviate ischemic brain injury after stroke (Chen et al., 2014). SIRT3 is an NAD^+ dependent deacetylase that mainly locates at mitochondria. SIRT3 acts to maintain mitochondrial homeostasis under a number of different stresses including cellular stress (Marcus and Andrabi, 2018). STI1 is a stress responsive factor that is involved in multiple intracellular and extracellular events for cellular protection against stress. STI1 could exert neuroprotection against ischemic insult by a mechanism involving increased secretion from astrocytes (Beraldo et al., 2013).

In this study, adenoviral vector was used to obtain higher transfection efficiency of OCT4B-190 *in vitro* and *in vivo*. Generally, adenoviral vectors are easy to be manipulated for genetic modification and have the capability to yield high titers. In addition, these vectors have a broad cell tropism and are rarely pathogenic to humans (Vujadinovic and Vellinga, 2018; Zhang and Zhou, 2016). With these advantages, the adenovirus- based delivery system has shown great prospects for clinical applications, especially in the exploring of recombinant vaccines and cancer therapeutics (Sayedahmed et al., 2019). However, adenoviral vectors have some limitations, such as the transient nature of

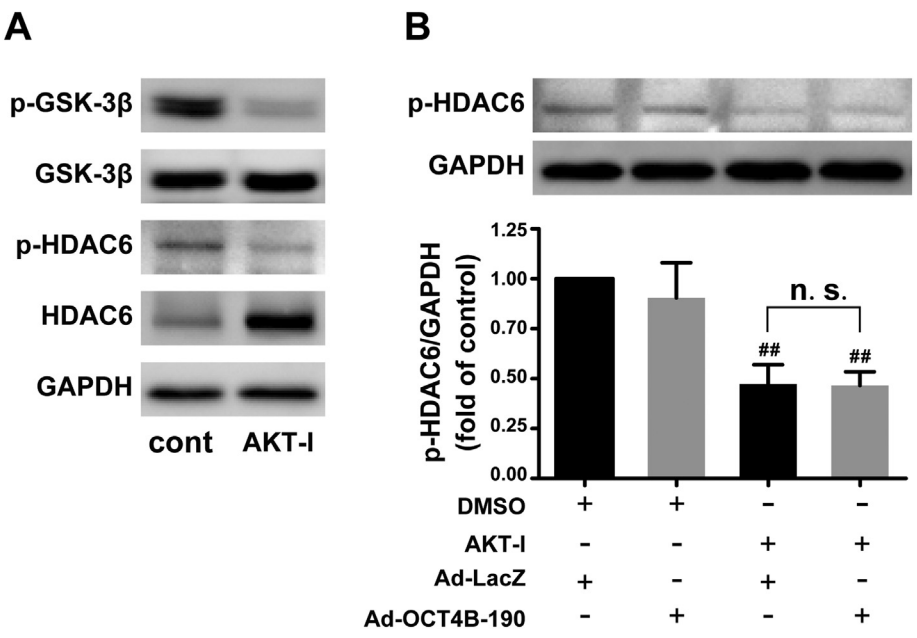

Supplementary Fig. 7. The independence of p-HDAC6 with GSK-3β kinase activation. Primary cortical neurons were infected with adenovirus expressing OCT4B-190 or control adenovirus for 3 days, and then neurons were subjected to DMSO or AKT inhibitor (AKT-I), 1 h after which the expression of GSK-3β and HDAC6 was examined by western blotting. **A.** Representative immunoblot of GSK-3β and HDAC6 from primary neuronal cultures. **B.** Representative immunoblot of p-HDAC6 after overexpression of OCT4B-190 from DMSO or AKT-I treated- neuronal cultures. Statistics results showed that OCT4B-190 overexpression did not affect the p-HDAC6 expression. Data are presented as means ± SEM. (n = 3), $^{\#\#}P < .01$ *vs.* control (neuronal cultures treated with DMSO), n.s. indicates no statistical difference between OCT4B-190 + AKT-I and AKT group.

transgene expression and the host immune response against viral antigens (Muruve, 2004; Sayedahmed et al., 2019). During the last decade, recombinant therapeutic proteins, an alternative delivery strategy for virus- based gene therapy, occupy a major portion of the approved drugs globally (Domanskyi et al., 2015; Goswami et al., 2018; Leader et al., 2008). However, there are still several challenges when using recombinant proteins as therapeutic drugs. Proteins do not always pass the blood brain barrier (BBB) and therefore should be delivered directly into the brain parenchyma. For the protein-based therapeutics, proper protein concentrations and delivery site should be carefully considered (Domanskyi et al., 2015).

5. Conclusions

This study for the first time revealed novel biological functions of OCT4B-190 in the experimental stroke, with implications for targeting GSK-3β and HDAC6 simultaneously as a possible neuroprotective strategy. Future efforts are needed to better explore more diverse effects of OCT4B isoforms, and to define the complicated actions and interrelations of HDAC6 and GSK-3β, which should provide the basis for the discovery of novel effective treatments for stroke.

Acknowledgements

This research was supported by the National Natural Science Foundation of China (81400971, 81630028, 81571135), the Nanjing Outstanding Youth Foundation (JQX16024), the Key Research and Development Program of Jiangsu Province of China (BE2016610), the Jiangsu Province Key Medical Discipline (ZDXKA2016020).

Conflict of interest

The authors declare no conflict of interest.

The following are the supplementary data related to this article.

References

Baltan, S., Murphy, S.P., Danilov, C.A., Bachleda, A., Morrison, R.S., 2011. Histone deacetylase inhibitors preserve white matter structure and function during ischemia by conserving ATP and reducing excitotoxicity. J. Neurosci. 31, 3990–3999.

Baxter, P., Chen, Y., Xu, Y., Swanson, R.A., 2014. Mitochondrial dysfunction induced by nuclear poly(ADP-ribose) polymerase-1: a treatable cause of cell death in stroke. Transl. Stroke Res. 5, 136–144.

Beraldo, F.H., Soares, I.N., Goncalves, D.F., Fan, J., Thomas, A.A., Santos, T.G., Mohammad, A.H., Roffe, M., Calder, M.D., Nikolova, S., Hajj, G.N., Guimaraes, A.L., Massensini, A.R., Welch, I., Betts, D.H., Gros, R., Drangova, M., Watson, A.J., Bartha, R., Prado, V.F., Martins, V.R., Prado, M.A., 2013. Stress-inducible phosphoprotein 1 has unique cochaperone activity during development and regulates cellular response to ischemia via the prion protein. FASEB J. 27, 3594–3607.

Borgas, D., Chambers, E., Newton, J., Ko, J., Rivera, S., Rounds, S., Lu, Q., 2016. Cigarette smoke disrupted lung endothelial barrier integrity and increased susceptibility to acute lung injury via histone Deacetylase 6. Am. J. Respir. Cell Mol. Biol. 54, 683–696.

Chang, L., Chen, Y., Li, J., Liu, Z., Wang, Z., Chen, J., Cao, W., Xu, Y., 2011. Cocaine-and amphetamine-regulated transcript modulates peripheral immunity and protects against brain injury in experimental stroke. Brain Behav. Immun. 25, 260–269.

Chen, S., Owens, G.C., Makarenkova, H., Edelman, D.B., 2010. HDAC6 regulates mitochondrial transport in hippocampal neurons. PLoS One 5, e10848.

Chen, Y.T., Zang, X.F., Pan, J., Zhu, X.L., Chen, F., Chen, Z.B., Xu, Y., 2012. Expression patterns of histone deacetylases in experimental stroke and potential targets for neuroprotection. Clin. Exp. Pharmacol. Physiol. 39, 751–758.

Chen, Y., Won, S.J., Xu, Y., Swanson, R.A., 2014. Targeting microglial activation in stroke therapy: pharmacological tools and gender effects. Curr. Med. Chem. 21, 2146–2155.

Chen, Y., Brennan-Minnella, A.M., Sheth, S., El-Benna, J., Swanson, R.A., 2015. Tat-NR2B9c prevents excitotoxic neuronal superoxide production. J. Cereb. Blood Flow Metab. 35, 739–742.

Chen, Y., Jin, Y., Zhan, H., Chen, J., Meng, H., Jin, J., Yu, L., Cao, X., Xu, Y., 2017. Proteomic analysis of the effects of Nur77 on lipopolysaccharide-induced microglial activation. Neurosci. Lett. 659, 33–43.

Domanskyi, A., Saarma, M., Airavaara, M., 2015. Prospects of Neurotrophic factors for Parkinson's disease: comparison of protein and gene therapy. Hum. Gene Ther. 26, 550–559.

Eltzschig, H.K., Eckle, T., 2011. Ischemia and reperfusion–from mechanism to translation. Nat. Med. 17, 1391–1401.

Ganai, S.A., 2017. Small-molecule modulation of HDAC6 activity: the propitious therapeutic strategy to vanquish neurodegenerative disorders. Curr. Med. Chem. 24, 4104–4120.

Gao, Y., Wei, J., Han, J., Wang, X., Su, G., Zhao, Y., Chen, B., Xiao, Z., Cao, J., Dai, J., 2012. The novel function of OCT4B isoform-265 in genotoxic stress. Stem Cells 30, 665–672.

George, P.M., Steinberg, G.K., 2015. Novel stroke therapeutics: Unraveling stroke pathophysiology and its impact on clinical treatments. Neuron 87, 297–309.

Goswami, D., Zhang, J., Bondarenko, P.V., Zhang, Z., 2018. MS-based conformation analysis of recombinant proteins in design, optimization and development of biopharmaceuticals. Methods 144, 134–151.

Guo, Y., Mantel, C., Hromas, R.A., Broxmeyer, H.E., 2008. Oct-4 is critical for survival/antiapoptosis of murine embryonic stem cells subjected to stress: effects associated with Stat3/survivin. Stem Cells 26, 30–34.

Hanumanthappa, P., Densi, A., Krishnamurthy, R.G., 2014. Glycogen synthase kinase-beta3 in ischemic neuronal death. Curr. Neurovasc. Res. 11, 271–278.

Jung, J.E., Kim, G.S., Chen, H., Maier, C.M., Narasimhan, P., Song, Y.S., Niizuma, K., Katsu, M., Okami, N., Yoshioka, H., Sakata, H., Goeders, C.E., Chan, P.H., 2010. Reperfusion and neurovascular dysfunction in stroke: from basic mechanisms to potential strategies for neuroprotection. Mol. Neurobiol. 41, 172–179.

Khanfar, M.A., Hill, R.A., Kaddoumi, A., El Sayed, K.A., 2010. Discovery of novel GSK-3beta inhibitors with potent in vitro and in vivo activities and excellent brain permeability using combined ligand- and structure-based virtual screening. J. Med.

Chem. 53, 8534–8545.
Langley, B., Brochier, C., Rivieccio, M.A., 2009. Targeting histone deacetylases as a multifaceted approach to treat the diverse outcomes of stroke. Stroke 40, 2899–2905.
Leader, B., Baca, Q.J., Golan, D.E., 2008. Protein therapeutics: a summary and pharmacological classification. Nat. Rev. Drug Discov. 7, 21–39.
Leng, Y., Liang, M.H., Ren, M., Marinova, Z., Leeds, P., Chuang, D.M., 2008. Synergistic neuroprotective effects of lithium and valproic acid or other histone deacetylase inhibitors in neurons: roles of glycogen synthase kinase-3 inhibition. J. Neurosci. 28, 2576–2588.
Liesz, A., Zhou, W., Na, S.Y., Hammerling, G.J., Garbi, N., Karcher, S., Mracsko, E., Backs, J., Rivest, S., Veltkamp, R., 2013. Boosting regulatory T cells limits neuroinflammation in permanent cortical stroke. J. Neurosci. 33, 17350–17362.
Lin, Y.H., Dong, J., Tang, Y., Ni, H.Y., Zhang, Y., Su, P., Liang, H.Y., Yao, M.C., Yuan, H.J., Wang, D.L., Chang, L., Wu, H.Y., Luo, C.X., Zhu, D.Y., 2017. Opening a new time window for treatment of stroke by targeting HDAC2. J. Neurosci. 37, 6712–6728.
Lin, S.C., Chung, C.H., Kuo, M.H., Hsieh, C.H., Chiu, Y.F., Shieh, Y.S., Chou, Y.T., Wu, C.W., 2019. OCT4B mediates hypoxia-induced cancer dissemination. Oncogene 38, 1093–1105 (Epub 2018 Sep 12).
Liu, X., Yamashita, T., Shang, J., Shi, X., Morihara, R., Huang, Y., Sato, K., Takemoto, M., Hishikawa, N., Ohta, Y., Abe, K., 2018. Molecular switching from ubiquitin-proteasome to autophagy pathways in mice stroke model. J. Cereb. Blood Flow Metab. 1–11. https://doi.org/10.1177/0271678X18810617.
Luo, X., Kraus, W.L., 2012. On PAR with PARP: cellular stress signaling through poly (ADP-ribose) and PARP-1. Genes Dev. 26, 417–432.
Marcus, J.M., Andrabi, S.A., 2018. SIRT3 regulation under cellular stress: making sense of the ups and downs. Front. Neurosci. 12, 799.
Matthias, P., Yoshida, M., Khochbin, S., 2008. HDAC6 a new cellular stress surveillance factor. Cell Cycle 7, 7–10.
Meng, L., Hu, H., Zhi, H., Liu, Y., Shi, F., Zhang, L., Zhou, Y., Lin, A., 2018. OCT4B regulates p53 and p16 pathway genes to prevent apoptosis of breast cancer cells. Oncol. Lett. 16, 522–528.
Muruve, D.A., 2004. The innate immune response to adenovirus vectors. Hum. Gene Ther. 15, 1157–1166.
Parmigiani, R.B., Xu, W.S., Venta-Perez, G., Erdjument-Bromage, H., Yaneva, M., Tempst, P., Marks, P.A., 2008. HDAC6 is a specific deacetylase of peroxiredoxins and is involved in redox regulation. Proc. Natl. Acad. Sci. U. S. A. 105, 9633–9638.
Patnala, R., Arumugam, T.V., Gupta, N., Dheen, S.T., 2017. HDAC inhibitor sodium butyrate-mediated epigenetic regulation enhances Neuroprotective function of microglia during ischemic stroke. Mol. Neurobiol. 54, 6391–6411.
Radzisheuskaya, A., Silva, J.C., 2014. Do all roads lead to Oct4? The emerging concepts of induced pluripotency. Trends Cell Biol. 24, 275–284.
Rajanahalli, P., Stucke, C.J., Hong, Y., 2015. The effects of silver nanoparticles on mouse embryonic stem cell self-renewal and proliferation. Toxicol. Rep. 2, 758–764.
Rana, A.K., Singh, D., 2018. Targeting glycogen synthase kinase-3 for oxidative stress and neuroinflammation: opportunities, challenges and future directions for cerebral stroke management. Neuropharmacology 139, 124–136.
Rivieccio, M.A., Brochier, C., Willis, D.E., Walker, B.A., D'Annibale, M.A., McLaughlin, K., Siddiq, A., Kozikowski, A.P., Jaffrey, S.R., Twiss, J.L., Ratan, R.R., Langley, B., 2009. HDAC6 is a target for protection and regeneration following injury in the nervous system. Proc. Natl. Acad. Sci. U. S. A. 106, 19599–19604.
Ryu, H.W., Won, H.R., Lee, D.H., Kwon, S.H., 2017. HDAC6 regulates sensitivity to cell death in response to stress and post-stress recovery. Cell Stress Chaperones 22, 253–261.
Sayedahmed, E.E., Kumari, R., Mittal, S.K., 2019. Current use of adenovirus vectors and their production methods. Methods Mol. Biol. 1937, 155–175.
Villodre, E.S., Kipper, F.C., Pereira, M.B., Lenz, G., 2016. Roles of OCT4 in tumorigenesis, cancer therapy resistance and prognosis. Cancer Treat. Rev. 51, 1–9.
Vujadinovic, M., Vellinga, J., 2018. Progress in adenoviral capsid-display vaccines. Biomedicines 6.
Wang, X., Zhao, Y., Xiao, Z., Chen, B., Wei, Z., Wang, B., Zhang, J., Han, J., Gao, Y., Li, L., Zhao, H., Zhao, W., Lin, H., Dai, J., 2009. Alternative translation of OCT4 by an internal ribosome entry site and its novel function in stress response. Stem Cells 27, 1265–1275.
Wang, Z., Leng, Y., Wang, J., Liao, H.M., Bergman, J., Leeds, P., Kozikowski, A., Chuang, D.M., 2016. Tubastatin A, an HDAC6 inhibitor, alleviates stroke-induced brain infarction and functional deficits: potential roles of alpha-tubulin acetylation and FGF-21 up-regulation. Sci. Rep. 6, 19626.
Wang, X.X., Wan, R.Z., Liu, Z.P., 2018. Recent advances in the discovery of potent and selective HDAC6 inhibitors. Eur. J. Med. Chem. 143, 1406–1418.
Wu, H., Cheng, X.W., Hu, L., Takeshita, K., Hu, C., Du, Q., Li, X., Zhu, E., Huang, Z., Yisireyili, M., Zhao, G., Piao, L., Inoue, A., Jiang, H., Lei, Y., Zhang, X., Liu, S., Dai, Q., Kuzuya, M., Shi, G.P., Murohara, T., 2016. Cathepsin S activity controls injury-related vascular repair in mice via the TLR2-mediated p38MAPK and PI3K-Akt/p-HDAC6 Signaling pathway. Arterioscler. Thromb. Vasc. Biol. 36, 1549–1557.
Zhang, C., Zhou, D., 2016. Adenoviral vector-based strategies against infectious disease and cancer. Hum. Vaccin. Immunother. 12, 2064–2074.
Zhu, X., Ye, L., Ge, H., Chen, L., Jiang, N., Qian, L., Li, L., Liu, R., Ji, S., Zhang, S., Jin, J., Guan, D., Fang, W., Tan, R., Xu, Y., 2013. Hopeahainol a attenuates memory deficits by targeting beta-amyloid in APP/PS1 transgenic mice. Aging Cell 85–92.
Zhu, X., Wang, S., Yu, L., Yang, H., Tan, R., Yin, K., Jin, J., Zhao, H., Guan, D., Xu, Y., 2014. TL-2 attenuates beta-amyloid induced neuronal apoptosis through the AKT/GSK-3beta/beta-catenin pathway. Int. J. Neuropsychopharmacol. 17, 1511–1519.